

Article

Theoretical Studies of Acrolein Hydrogenation to Propenol and Propanal on Au₃ and Au₅

Guo-Jun Kang¹, Shuai He¹ and Xue-Feng Ren^{1,2,*}

¹ Low Carbon Energy Institute, School of Chemical Engineering & Technology, China University of Mining & Technology, Xuzhou 221008, China; gjkang@cumt.edu.cn (G.-J.K.); kingfeng030611@163.com (S.H.)

² Fukui Institute for Fundamental Chemistry, Kyoto University, 34-4 Takano Nishihiraki-cho, Sakyo, Kyoto 606-8103, Japan

* Correspondence: renxf@cumt.edu.cn

Abstract: The stepwise hydrogenation of the C=C bond and C=O group of acrolein on Au₃ and Au₅ model systems is investigated using the density functional theory(DFT) PW91 functional. Our results show that the C=C hydrogenation is more favorable than that of C=O bond on Au₃ with the barriers of the rate-determining step being 0.35 and 0.62 eV respectively. On the other hand, the C=O reduction is preferred over the hydrogenation of the C=C bond on Au₅. The corresponding barriers of the rate-determining steps are 0.45 and 0.54 eV, respectively. This demonstrated that the second hydrogenation step controls the reaction on both Au₃ and Au₅ for C=O and C=C hydrogenation and the C=O hydrogenation on Au₅ is preferred over the hydrogenation of the C=C bond, which is helpful to address the reactivity of small size-selected supported gold clusters.

Keywords: acrolein; Au Cluster; DFT

1. Introduction

Unsaturated alcohols which are a kind of important chemical intermediates used to synthesize pharmaceuticals and flavoring material[1, 2] are usually produced via selective hydrogenation of α , β -unsaturated aldehydes. Normally the C=C bond is more active than the C=O bond both thermodynamically and kinetically[3]. Acrolein is the smallest α , β -unsaturated aldehyde molecule containing conjugated C=C and C=O double bond, and is used as a probe molecule to study the hydrogenation activity toward the C=C and C=O bonds on the Ag[4-7], Pt[8-11], Ni/Pt(111)[12, 13] surface both experimentally and theoretically. However, the selective hydrogenation of acrolein to propenol is considered the most difficult one and the selectivity to unsaturated alcohols on conventional catalysts of group VIII metals is generally low (~2% on Pt)[9]. It is a challenging task to increase the selectivity for the unsaturated alcohols with respect to the saturated aldehydes.

Recently gold exhibits unexpected activity for the selective hydrogenation of α , β -unsaturated aldehydes to unsaturated alcohols.[14-17] Experimental studies substantiated the crucial role of Au as an active component in the selective hydrogenation. But the periodic density functional calculation of our group showed that acrolein is very weakly adsorbed on the clean regular Au(111) or the flat Au(110) surface[18]. A higher selectivity had been obtained on supported gold nano-particles[9]. Gold supported on TiO₂, Al₂O₃ or SiO₂ was demonstrated to catalyze alkene hydrogenation, and it was suggested that small gold clusters were the catalytically active species.[14, 15]

Although there are already many studies in the literature about the selective hydrogenation of acrolein on the different metal surfaces and supported metal catalysts, little information is known

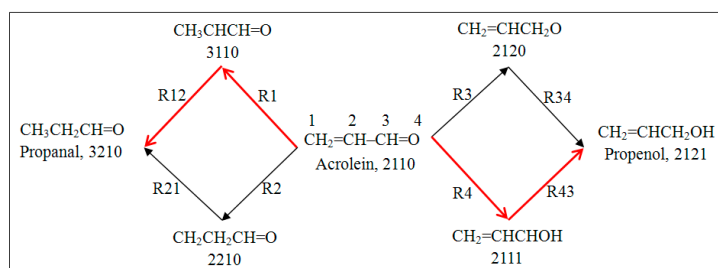
about acrolein hydrogenation on the gold clusters. No doubt, a comprehensive knowledge of hydrogenation of acrolein on the gold cluster is very instructive for improving the performance of the known noble metal catalysts and for screening new and better candidates. In this paper, we address acrolein hydrogenation on Au clusters. The whole paper is arranged as follows. The favorable pathways of C=C and C=O hydrogenation on Au₃ and Au₅ are discussed in detail in Part II. Computational methods are presented in Part III. Finally, the conclusions are presented in Part IV.

2. Results and discussion

2.1. Acrolein hydrogenation on Au₃

2.1.1. Hydrogenation of the C=C bond

Acrolein hydrogenation is believed to follow the Houriti-Polanyi mechanism[19]. We have investigated adsorption and dissociation of H₂ molecule on gold clusters and found that H₂ dissociation can take place on Au₃ and Au₅[20] and acrolein binds to Au₃ and Au₅ via the most strongly in di-σ-(C, O) mode with the binding energy of 1.52 eV and 1.43 eV respectively[21]. Thus, we investigated acrolein hydrogenation on gold clusters using Au₃ and Au₅ as representative models. Theoretically there are various hydrogenation products on the gold clusters. Now we use klmn to denote these species. Here k, l, m and n are integers which represent the number of H atom bonding to C1, C2, C3 and O atoms of acrolein, respectively. The atom numbering of acrolein is C1–C2–C3–O4 (scheme1). For example, acrolein (2110) means that there are two, one and one H atoms bonded to C1, C2 and C3 atoms, respectively, and the O atom has no H atom[22]. We confined our study to stepwise hydrogenation that produce the desired product propenol (2121) and the main undesired side product propanal (3210) through route 43 (R43) and route 12 (R12) (Route nm means that the first H atom attacks at the nth atom and the second H at mth atom. For the ordering of atoms, please see Scheme 1), respectively. In principle, there are other pathways to propenol such as R34(R21). However, according to the well-accepted mechanism and our located co-adsorption structures, these routes are excluded because the co-adsorbed H atoms sit quite far away from the attacked atom (C3 or C2 respectively). It should be pointed out there are various initial states with different stability as shown in Figure A1-A4 in supporting information. However, only those from the most stable initial states are investigated here.



Scheme 1. Reaction pathway of acrolein hydrogenation forming the propanal and propenol. The optimal mechanism is marked in red on the Au₃ and Au₅.

Figure 1 shows the most stable precursor structure for the hydrogenation of the C=C bond in which the attacking H atom and the attacked C1 atom are sitting at the same gold atom (Figure 1, 3IS₁) with H-Au bond length of 1.61 Å. Compared to di-σ-(C, O)/Au₃[21], the C1-Au bond length of 3IS₁ is elongated from 2.17 Å to 2.34 Å and C1-C2 bond is stretched by 0.03 Å. The O-Au, C₃-O and

C2-C3 bond lengths vary within 0.01 Å. In this precursor structure, the H atom can only attack C1 atom. Therefore the hydrogenation route of C=C bond follows route 12. Attacking of the H atom to C1 leads to the 3TS₁ transition state structure. In the 3TS₁, the H atom is basically located between C1 and the Au, which results in a elongated C1-Au bond distance of 3.00 Å, compared to 2.34 Å in 3IS₁. Correspondingly the C1-H bond reduces from 2.83 Å in 3IS₁ to 1.80 Å in 3TS₁. Generally speaking, the framework bonds change little in 3TS₁ with respect to the corresponding values in 3IS₁ (Figure 1). After the 3TS₁, the reaction results in an intermediate product 3IM_{1A}. In this structure, the framework changes a lot. For example, the C1-C2 bond is extended to 1.51 Å while the C2-C3 bond is shortened by 0.05 Å, compared with 3TS₁. The H-C1 bond is formed with the bond length of 1.11 Å. The produced intermediate adsorbs on Au₃ mainly through O interaction with the substrate by the O-Au bond reduced from 2.13 Å to 2.04 Å.

Table 1. Energy barriers and reaction energies of the first and second step of acrolein hydrogenation on Au₃ and Au₅. The energy of each initial state (IS) is taken as zero energy reference.

step	Au ₃ E (eV)		Au ₅ E (eV)		step	Au ₃ E (eV)		Au ₅ E (eV)	
	C=C					C=O			
1 st	3IS ₁	0	5IS ₁	0	1 st	IS ₄	0.00	5IS ₁	0
	3TS ₁	0.29	5TS ₁	0.30		3TS ₄	0.94	5TS ₄	0.17
	3IM _{1A}	0.04	5IM _{1A}	-0.34		3IM _{4A}	0.48	5IM _{4A}	-0.27
	3IM _{1B}	-0.38	5IM _{1B}	-1.10		3IM _{4B}	0.16	5IM _{4B}	-0.66
2 nd	3IS ₁₂	0	5IS ₁₂	0	2 nd	3IS ₄₃	0	5IS ₄₃	0
	3TS ₁₂	0.35	5TS ₁₂	0.54		3TS ₄₃	0.62	5TS ₄₃	0.45
	3FS ₁₂	0.02	5FS ₁₂	-0.62		3FS ₄₃	-0.38	5FS ₄₃	-0.25

A lot of calculations demonstrate species with unpaired electrons interact with the substrates favorably through the atom with its unpaired electron. However, 3IM_{1A} is not the most stable adsorption complex and it adsorbs through C1 and O4, not C2 which has an unpaired electron. We found that 3IM_{1B} is the most stable adsorption configuration. Conversion 3IM_{1A} to the most stable complex of 3IM_{1B} releases the heat of 0.34 eV (Table 1). In 3IM_{1B}, the H-Au bond is broken and the C2-Au bond is formed with a bond distance of 2.23 Å which is shorter by 0.11 Å than C1-Au in 3IS₁. Because of stronger interaction of C2 and Au, C2-C3 bond is weakened and increases from 1.39 Å to

1.46 Å. Simultaneously, the O-Au bond and Au-Au bond increase 0.11 Å and 0.10 Å, respectively.

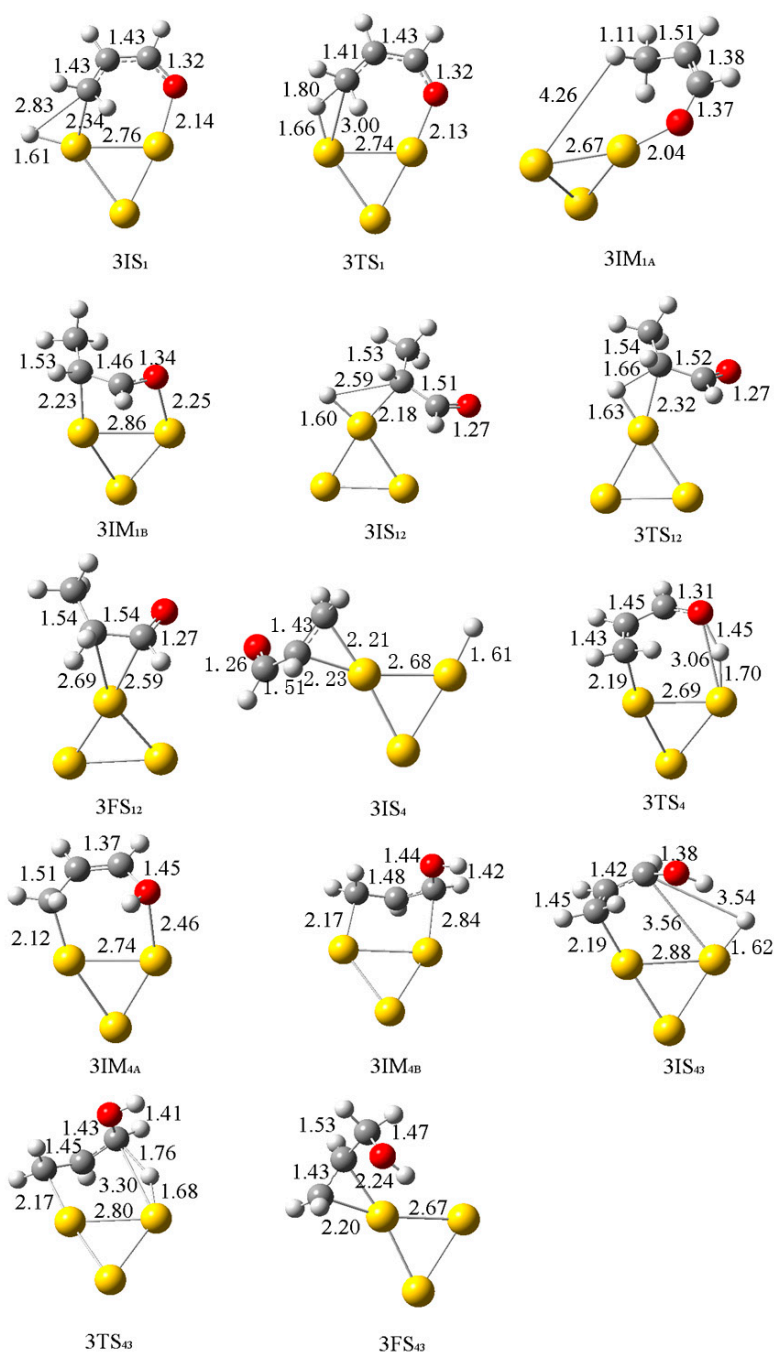


Figure 1. Adsorption geometries of acrolein hydrogenation on the Au_3 calculated at PW91/cep-121G level.

The next step of hydrogenation of the C=C bond along route 12 is addition of H atom at C2. The co-adsorption of H atom and 3110 on the Au_3 is shown in Figure 1. Like 3IS₁, the H atom and the C2 atom also share the gold atom in 3IS₁₂. In this co-adsorption structure, 3110 practically binds to Au_3 via C2-Au interaction. The C2-Au distance, 2.18 Å, is significantly shorter than 2.34 Å in 3IS₁. In the 3TS₁₂, the H atom, C2 and the Au form a triangle structure. In the transition state 3TS₁₂, the H-Au bond length is 1.63 Å and the C2-H bond distance decreases from 2.59 Å to 1.66 Å. However, C1-C2, C2-C3 and C=O bond lengths are almost unchanged. This shows that the influence of H attacking at

C2 is relatively local. Product 3210 is saturated aldehyde and interacts with Au₃ via C2-Au (2.69 Å) and C3-Au (2.59 Å) interaction. Note the corresponding C1-C2 bond length and C2-C3 bond length are equal and is close to the C-C bond length of ethane (1.55 Å) at the same level. This is understandable because C1 and C2 are "saturated". Kinetically, the energy barrier of 12 pathway is 0.35 eV, which shows that C=C hydrogenation on Au₃ is likely (Table 1).

2.1.2. Hydrogenation of the C=C bond

3IS₄ is the initial state used for the first step of C=O hydrogenation. To attack the O atom of 3IS₄, the H atom first rotates which weakens the O-Au bonding in the di-σ-(C, O)-cis-AC mode[21]. In the 3TS₄, the H atom is between the O atom and the Au with the O-H and H-Au bond lengths of 1.45 and 1.70 Å respectively (Figure 1). The variation of C1-C2, C2-C3, C3-O and C1-Au is within 0.02 Å. Moreover, the Au-Au bond varies from 2.68 Å to 2.69 Å, indicating a slightly stabilizing deformation of Au₃. In addition, O-Au bond is decrease from 5.95 Å in 3IS₄ to 3.06 Å in 3TS₄, which shows that the O-Au bond is also broken and the O atom does not interact with Au₃ directly.

As in the C=C hydrogenation, an intermediate product, 3IM_{4A}, is also formed firstly (Figure 1). In this case, the O-Au bond length is 2.46 Å, indicating that O-Au bond is formed. The H-Au bond is broken. 3IM_{4A} is also not stable enough to be the final product because the saturated O atom produces an unpaired electron on C3, which makes C3 possess strong bonding ability. Transformation of 3IM_{4A} into 3IM_{4B} releases the heat of 0.32 eV.

Based on the 3IM_{4B}, we studied the second step of C=O hydrogenation. 3IS₄₃ shown in Figure 1 illustrates the initial structure (co-adsorptions structure) of H with 2111, the product of the first hydrogenation. The H-Au bond length is 1.62 Å. The C2-Au distance is elongated from 2.84 Å of 3IM_{4B} to 3.56 Å. In the 3TS₄₃ the H atom links C3 and the Au with H-Au and H-C3 being 1.68 and 1.76 Å respectively. As shown in Figure 1, the C3-O bond is elongated by 0.03 Å due to H addition. The hydrogenation product 3FS₄₃ is 2121. Because the C=O bond is hydrogenated, the C2-C3 bond length (1.53 Å) and C3-O bond length (1.47 Å) in 3FS₄₃ are close to the C-C single bond length in ethane (1.55 Å) and C-O bond length in methanol. C1-C2 bond length is 0.07 Å longer than C=C double bond length (1.36 Å) of the isolated acrolein. As shown in Figure 1, 2121 interacts with gold atom via π-C=C mode. The C=O hydrogenation reaction on Au₃ is an exothermic reaction with a reaction heat of 0.38 eV, which implies that C=O hydrogenation on Au₃ is favorable thermodynamically. However, the energy barrier of 43 pathway (0.94 eV) is higher than that of 12 pathway (0.35 eV), which indicates that on Au₃ C=C hydrogenation is more favorable than C=O hydrogenation.

2.2. Acrolein hydrogenation on Au₅

The most stable coadsorption structures of 2110 and H atom on Au₅ were chosen as initial states (5IS₁) for C=C and C=O hydrogenation (Figure 2). In the 5IS₁, acrolein interacts directly with Au₅ via C-Au bond (2.21 Å) and O-Au bond (2.17 Å). The H atom locates at the middle of Au-Au bond that can directly interact with 2110 and the corresponding C1-H and O-H bond length is 2.55 Å and 2.50 Å as shown in Figure 2.

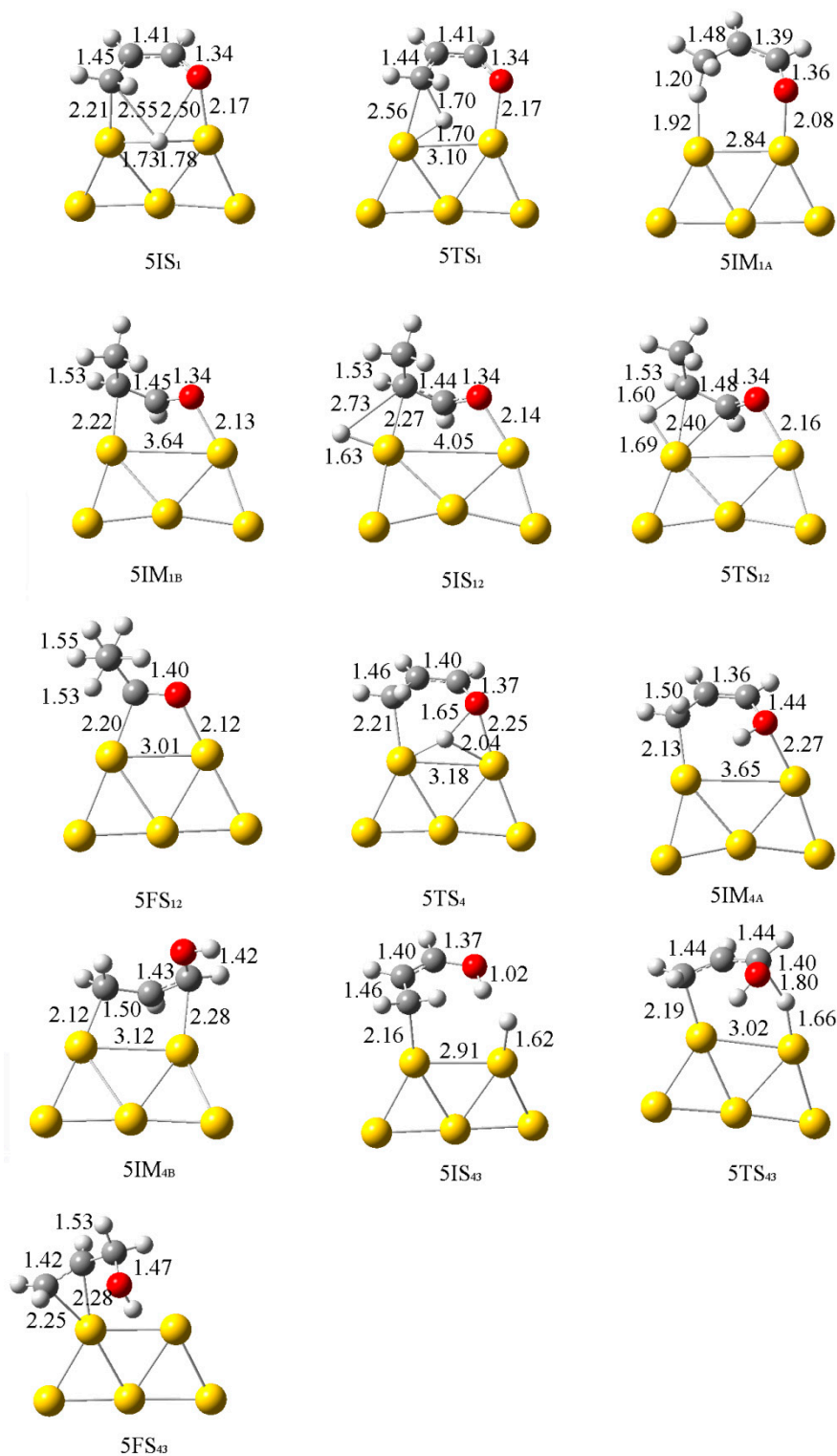


Figure 2. Adsorption geometries of acrolein hydrogenation on the Au₅ calculated at PW91/cep-121G level.

2.2.1. Hydrogenation of the C=C bond

At the beginning of this reaction, the H atom moves toward the C1 atom, accompanied by elongation of C1-Au bond. This motion eventually allows the H atom to insert into C1-Au bond of 5IM_{1A} (Figure 2). In 5TS₁, the C1-Au, C1-H and the H-Au length are 2.56, 1.70 and 1.70 Å, respectively. The triangle containing C1, the H and Au atoms are formed. The C1-Au bond increases

from 2.21 Å to 2.56 Å in the 5TS₁. The C1-C2, C2-C3, C3-O and O-Au vary slightly (within 0.01 Å), indicating that the influence of H attacking at C1 atom is relatively local in the first step of C=C bond hydrogenation. In the intermediate of 5IM_{1A} (3110), the Au-H bond and the C1-H bonds are 1.92 Å and 1.20 Å respectively. The C1 atom cannot interact directly with Au₅. Hydrogenation of C1 produces a radical centered on C2 atom. However, in 5IM_{1A} C2 does not interact with Au₅ directly. Thus, 5IM_{1A} is not stable and can convert into more stable 5IM_{1B}. Our calculated result indicates that this conversion is exothermic by 0.76 eV. In 5IM_{1B}, 3110 interacts with Au₅ by both C2-Au (2.22 Å) and O-Au bond (2.13 Å). Second hydrogenation starts from 5IS₁₂. Attacking of the H to C2 site results in the transition state 5TS₁₂. In the 5TS₁₂, the H-C2 distance is 1.60 Å and the C2-Au bond distance is 2.40 Å. In 5FS₁₂, the C=O bond of 3210 directly interacts with Au₅ in the di-σ-C=O mode with the C3-Au bond length of 2.20 Å and O-Au bond length of 2.12 Å. Because C=C bond is saturated by H atoms, C1-C2 bond length in 5FS₁₂ is 1.55 Å and is equal to that in ethane, accompanied by an elongation of C2-C3 bond from 1.44 Å in 5IS₁₂ to 1.53 Å. The rate-determining step of C=C hydrogenation reaction on Au₅ is exothermic by 0.62 eV with a low energy barrier of 0.54 eV.

2.2.2. Hydrogenation of the C=O bond

The first step of C=O hydrogenation also begins with 5IS₁. This reaction (from 5TS₄ to 5IM_{4A}) starts with the H atom approaching toward to the O-Au bond, which increases the O-Au distance from 2.17 Å in 5IS₁ to 2.25 Å in 5TS₄, indicating that the O-Au bond is weakened. Similar to the transition state 3TS₄, the H-Au bond length is 2.04 Å and the O-H distance is 1.65 Å in the 5TS₄. The C-O distance increases from 1.34 Å in 5IS₁ to 1.37 Å in 5TS₄. However, C1-Au, C1-C2 and C2-C3 bond lengths are almost unchanged (within 0.01 Å). This shows that the influence of H attacking at O is relatively local.

In the final state, 5IM_{4A}, the O-Au bond is 2.27 Å, indicating that the O-Au interaction is still significant. Unlikely 5IM_{1A}, 5IM_{4A} can interact directly with Au₅ via O-Au bond. Because hydrogenation at the O atom, the C3 atom of C=O bond becomes a radical. Thus, a stable adsorption structure should involve C3. Our computation indicates that 5IM_{4B} is 0.39 eV more stable than 5IM_{4A}. In 5IM_{4B}, the C3-Au bond distance is 2.28 Å in the 5IM_{4B}, and the product 2111 is stabilized by both C1-Au and C3-Au bonding. The second step of C=O hydrogenation begins with coadsorption state (5IS₄₃) of H atom and 2111. In the initial state (5IS₄₃) the H atom sits at the top site of a Au atom with H-Au distance of 1.62 Å. Due to the H-Au bond, the C3-Au bond no longer exists. In the TS structure 5TS₄₃, the H-C3 is 1.80 Å and the H-Au bond is elongated from 1.62 to 1.66 Å, showing that the H-Au interaction is only slightly weakened. The final product is 2121 (5FS₄₃). It adsorbs on Au₅ via the π-C=C- mode. The rate-determining step of the C=O hydrogenation reaction on Au₅ is an exothermic reaction with a reaction heat of -0.25 eV. The energy barrier is 0.45 eV. Compared to the barrier of C=C hydrogenation on Au₅, we can conclude that on Au₅ C=O hydrogenation is more favorable than C=C hydrogenation kinetically.

2.3. Competition of the C=C and C=O hydrogenation

Figure 3 and Figure 4 summaries the PES for the C=C and C=O hydrogenation on Au₃ and Au₅. The calculated barrier for the first and second steps of the C=C bond hydrogenation of acrolein (R12 pathway) are 0.29 (3TS₁) and 0.35 (3TS₁₂) eV. These two barriers are close to each others, though the latter is slightly higher than the former. Both reactions are essentially neutral with the endothermicity of less than 0.05 eV. Note the co-adsorbed intermediate 3IM_{1B} with H (0.56 eV) is

more stable than the precursor 3IS₁₂. Therefore, thermodynamically the second step is more difficult and thus, control the production of 3210, the product of the C=C bond hydrogenation.

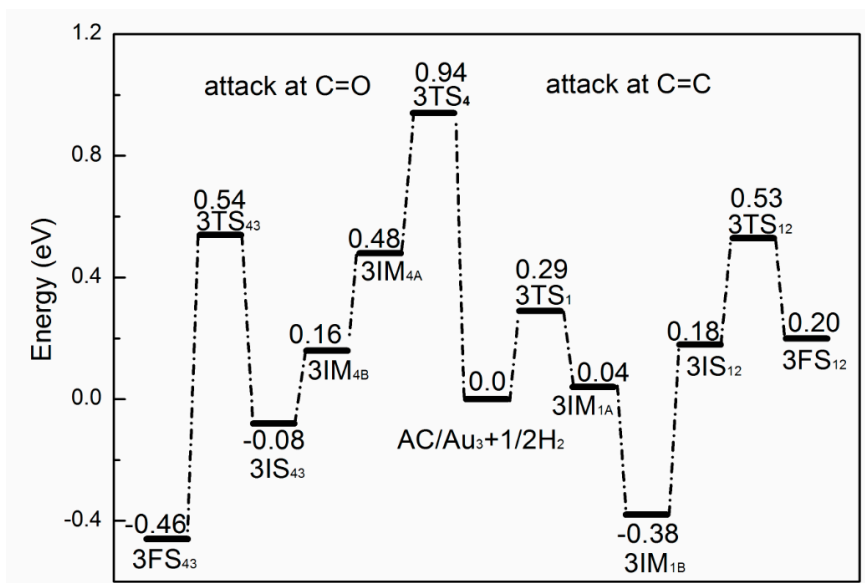


Figure 3. Pathways of acrolein(AC) hydrogenation on Au₃. The energies of the IS plus half of the energy of an isolated H₂ molecule is taken as the zero energy reference point (AC/Au₃+1/2H₂). All the energies of IMs and TSs for the first step are referred to the energies of the adsorbed structure together with half of the energy of the free H₂ molecule.

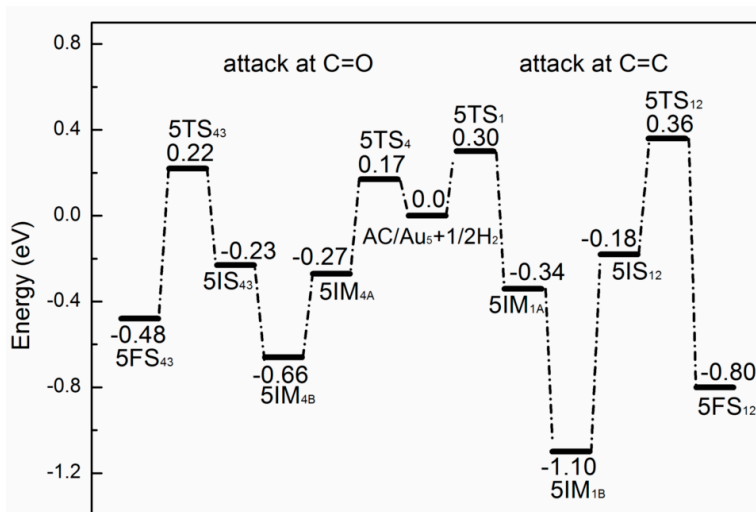


Figure 4. Pathways of acrolein(AC) hydrogenation on Au₅. The energies of the IS plus half of the energy of an isolated H₂ molecule is taken as the zero energy reference point (AC/Au₅+1/2H₂)

On the other hand, the barrier for the C=O hydrogenation are 0.94 (3TS₄) and 0.62 (3TS₄₃) eV, which are also similar to the step hydrogenation of C=C bond on Au₃ (Figure 3). The first step to 3IM_{4A} is endothermic whereas conversion to the most stable structure releases heat of 0.48 eV. The second hydrogenation step lowers the energy of the system by 0.46 eV.

Compared with the energy barrier of 12, we found that C=C hydrogenation with the highest energy barrier of 0.35 eV, is more favorable than C=O hydrogenation with the highest barrier of 0.94 eV. This result is in agreement with the experimental observation that the yield of C=C reduction is higher than that of the C=O hydrogenation.

The stepwise hydrogenation barriers of C=C bond on Au₅ are 0.30 (5TS₁) and 0.54 eV (Figure 4) respectively. The most stable intermediate 5IM_{1B} is almost 1 eV lower in energy than the precursor 5IS₁₂, indicating that formation of 5IS₁₂ is thermodynamically less likely. Thus, the second step is the rate-limiting step. Both reactions are exothermic, > 0.3 eV (Figure 4). For the C=O hydrogenation (43 pathway), the corresponding energy barriers are 0.17 and 0.45 eV, which also shows that the second step is rate-determining step. The calculated results show that C=O hydrogenation barriers is slightly lower than the corresponding values for the C=C hydrogenation, indicating that C=O reduction is preferred on Au₅.

2.4 Comparison of acrolein hydrogenation on Au₃ and Au₅

Above we discussed the kinetics of C=C and C=O hydrogenation on Au₃ and Au₅ clusters respectively. Now we compare the C=C hydrogenation on Au₃ and Au₅. The energy barrier of 3TS₁ (0.29 eV on Au₃) for the first hydrogenation step is almost equal to that of 5TS₁ (0.30 eV on Au₅). However, the energy barrier of 5TS₁₂ (0.54 eV on Au₅) is 0.19 eV higher than that of 3TS₁₂ (0.35 eV on Au₃), indicating that the energy barrier of C=C hydrogenation increases from Au₃ to Au₅.

For C=O hydrogenation on Au₃ and Au₅, the calculated energy barrier of 3TS₄ (0.94 eV) in the first step is 0.77 eV higher than that of 5TS₄ (0.17 eV). Moreover, in the second step, the energy barrier of 3TS₄₃ (0.62 eV) is 0.17 eV higher than that of 5TS₄₃ (0.45 eV). These results indicate that the energy barrier of C=O hydrogenation decreases from Au₃ to Au₅.

To recap, C=C hydrogenation is favored on Au₃ (the energy barrier of the rate-limiting step: 0.35 eV for C=C vs 0.94 eV for C=O) while the C=O hydrogenation is preferred on Au₅ (0.45 eV for C=O vs. 0.54 eV for C=C). These facts indicate that the selectivity of acrolein hydrogenation has close relationship with cluster size, which is consistent with the experiments observation that the activity and selectivity to the desired unsaturated alcohol depends on particle size and increases with increasing particle size[17,23-24].

In addition, we also compare the comparison of acrolein hydrogenation on Au(110) and Au₂₀ clusters.

3 Models and computational details

Calculations were performed using generalized gradient functional PW91[25, 26] implemented in Gaussian 03 program package.[27] We used the effective core potential (ECP) basis set, cep-121G (6D, 10F) for Au, C and O,[28, 29] and a triple zeta basis set for H.[30] Frequency calculations were performed to characterize all the optimized structures to be local minima or transition states on the potential energy surfaces. The intrinsic reaction coordinate calculations were further carried out to ensure that the obtained transition states connect the right reactants and products.

4 Conclusion

The selective hydrogenation acrolein on the small gold cluster Au₃ and Au₅ is investigated using density functional theory PW91 functional. The mechanism is explored along two pathways: hydrogenation of C=C bond and C=O group. We show that on Au₃ C=C hydrogenation is more favorable than that of C=O bond with the corresponding barrier of rate-determining step of 0.35 eV vs 0.94 eV. On the other hand, on Au₅, C=O reduction is favored than hydrogenation of C=C bond. The corresponding barriers of the rate-determining steps are 0.45 and 0.54 eV, respectively.

Comparison of the present results on Au₃ and Au₅ indicated that the large particles favor the C=O hydrogenation, which is consistent with the experiments observation.

Supplementary Materials: The following are available online at www.mdpi.com/link, Figure A1: Potential energy surfaces of first hydrogenation step of acrolein on Au₃, Figure A2: Potential energy surfaces of second hydrogenation step of acrolein on Au₃, Figure A3: Potential energy surfaces of first hydrogenation step of acrolein on Au₅, Figure A4: Potential energy surfaces of second hydrogenation step of acrolein on Au₅.

Acknowledgments: Financial supports from the Fundamental Research Funds for the Central Universities (No. 2013QNA14). We are grateful to the High Performance Computing Center of China University of Mining and Technology for the award of CPU hours to accomplish this work. We would like to thank Prof. Zhaoxu Chen for many stimulating discussions.

Author Contributions: Guo-Jun Kang performed the calculation work and wrote the paper work. Shuai He collected and analyzed the calculated results; Xue-Feng Ren revised the paper.

Conflicts of Interest: The authors declare no conflict of interest.

References

- [1] Gallezot, P.; Richard D Selective Hydrogenation of α,β -Unsaturated Aldehydes, *Cat. Rev. Sci. Eng.* **1998**, *40*, 81-126.
- [2] Marinelli, T.B.L.W; Nabuurs, S.; Ponec, V. Activity and Selectivity in the Reactions of Substituted α,β -Unsaturated Aldehydes *J. Catal.* **1995**, *151*, 431-438.
- [3] Claus, P. Selective hydrogenation of α,β -unsaturated aldehydes and other C=O and C=C bonds containing compounds, *Top. Catal.* **1998**, *5*, 51-62.
- [4] Brandt, K.; Chiu, M.E.; Watson, D.J.; Tikhov, M.S.; Lambert RM Chemoselective Catalytic Hydrogenation of Acrolein on Ag(111): Effect of Molecular Orientation on Reaction Selectivity, *J. Am. Chem. Soc.* **2009**, *131*, 17286-17290.
- [5] Lim, K.H.; Mohammad, A.B.; Yudanov, I.V.; Neyman, K.M.; Bron, M.; Claus, P.; Rösch, N. Mechanism of Selective Hydrogenation of α,β -Unsaturated Aldehydes on Silver Catalysts: A Density Functional Study, *J. Phys. Chem. C* **2009**, *113*, 13231-13240.
- [6] Lim, K.H.; Chen, Z.X.; Neyman, K.M.; Rosch, N.; Adsorption of acrolein on single-crystal surfaces of silver: Density functional studies, *Chem. Phys. Lett.* **2006**, *420*, 60-64.
- [7] Ferullo, R.M.; Marta Branda, M.; Illas, F. Structure and stability of acrolein and allyl alcohol networks on Ag(111) from density functional theory based calculations with dispersion corrections, *Surf. Sci.* **2013**, *617*, 175-182.
- [8] Kliewer, C.J.; Bieri, M.; Somorjai, G.A. Hydrogenation of the α,β -Unsaturated Aldehydes Acrolein, Crotonaldehyde, and Prenal over Pt Single Crystals: A Kinetic and Sum-Frequency Generation Vibrational Spectroscopy Study, *J. Am. Chem. Soc.* **2009**, *131*, 9958-9966.
- [9] Loffreda, D.; Delbecq, F.; Vigne, F.; Sautet, P. Chemo-Regioselectivity in Heterogeneous Catalysis: Competitive Routes for CO and CC Hydrogenations from a Theoretical Approach, *J. Am. Chem. Soc.* **2006**, *128*, 1316-1323.
- [10] Marinelli, T.B.L.W; Ponec, V. A Study on the Selectivity in Acrolein Hydrogenation on Platinum Catalysts: A Model for Hydrogenation of α,β -Unsaturated Aldehydes *J. Catal.* **1995**, *156*:51-59.
- [11] Pirillo, S.; López-Corral, I.; Germán, E.; Density Functional Study of Acrolein Adsorption on Pt(111), *Juan, A.* **2014**, *99*, 259– 264.
- [12] Murillo, L. E.; Menning, C.A.; Chen, J.G. Trend in the Cdouble bond; length as m-dashC and Cdouble bond; length as m-dashO bond hydrogenation of acrolein on Pt-M (M = Ni, Co, Cu) bimetallic surfaces, *J. Catal.* **2009**, *268*, 335-342.

- [13] Luo, Q.; Wang, T.; Beller, M.; Jiao, H. Acrolein Hydrogenation on Ni(111) *J. Phys. Chem. C* **2013**, *117*, 12715-12724.
- [14] Claus, P. Heterogeneously catalysed hydrogenation using gold catalysts, *Appl. Catal. A Gen.* **2005**, *291*, 222-229.
- [15] Claus, P.; Hofmeister, H.; Mohr, C. Identification of active sites and influence of real structure of gold catalysts in the selective hydrogenation of acrolein to allyl alcohol *Gold. Bull.* **2004**, *37*, 181-186.
- [16] Milone, C.; Crisafulli, C.; Ingoglia, R.; Schipilliti, L.; Galvagno, S. A comparative study on the selective hydrogenation of α,β unsaturated aldehyde and ketone to unsaturated alcohols on Au supported catalysts, *Catal. Today*, **2007**, *122*, 341-351.
- [17] Mohr, C.; Hofmeister, H.; Radnik, J.; Claus, P. Identification of Active Sites in Gold-Catalyzed Hydrogenation of Acrolein, *J. Am. Chem. Soc.* **2003**, *125*, 1905-1911.
- [18] He, X.; Chen, Z.X.; Kang, G.J. Theoretical Study of the Role of Indium on the Selectivity of Acrolein Hydrogenation to Propenol on Gold Surfaces, *J Phys. Chem. C* **2009**, *113*, 12325-12330.
- [19] Horiuti, J.; Polanyi, M. Exchange reactions of hydrogen on metallic catalysts *Trans. Faraday. Soc.* **1934**, *30*, 1164-1172.
- [20] Kang, G.J.; Chen, Z.X.; Li, Z.; He, X. A theoretical study of the effects of the charge state and size of gold clusters on the adsorption and dissociation of H-2 *J. Chem. Phys.* **2009**, *130*, 034701-034706.
- [21] Kang, G.-J.; Chen, Z.-X.; Li, Z. Acrolein Adsorption on Gold Clusters, A Theoretical Study of Conjugation Effect on C=C and C=O Interaction with Au Clusters, *Catal. Lett.* **2011**, *141*, 996-1003.
- [22] Kang, G.-J.; Ma, J.; Chen, Z.-X. Theoretical Studies of Species Related to Acrolein Hydrogenation, *Catal. Lett.* **2012**, *142*, 287-293.
- [23] Claus, P.; Brückner, A.; Mohr, C.; Hofmeister, H. *J. Am. Chem. Soc.* **2000**, *122*, 11430-11439.
- [24] Mohr, C.; Hofmeister, H.; Claus, P. The influence of real structure of gold catalysts in the partial hydrogenation of acrolein *J. Catal.* **2003**, *213*, 86-94.
- [25] Perdew, J.P.; Chevary, J.A.; Vosko, S.H.; Jackson, K.A.; Pederson, M.R.; Singh, D.J.; Fiolhais, C. Atoms, molecules, solids, and surfaces: Applications of the generalized gradient approximation for exchange and correlation *Phys. Rev. B* **1992**, *46*, 6671-6687.
- [26] Perdew, J.P.; Chevary, J.A.; Vosko, S.H.; Jackson, K.A.; Pederson, M.R.; Singh, D.J.; Fiolhais, C. Erratum: Atoms, molecules, solids, and surfaces: Applications of the generalized gradient approximation for exchange and correlation, *Phys. Rev. B* **1993**, *48*, 4978(E).
- [27] Frisch, M.J.; Trucks, G.W.; Schlegel, H.B.; Scuseria, G.E.; Robb, M.A. (2004) Gaussian 03, Revision D.01, Gaussian, Inc., Wallingford CT, 2004.
- [28] Stevens, W.J.; Basch, H.; Krauss, M. Compact effective potentials and efficient shared-exponent basis sets for the first- and second-row atoms, *J Chem. Phys.*, **1984**, *81*, 6026-6033.
- [29] Stevens, W.J.; Krauss, M.; Basch, H.; Jasien, P. G. Relativistic compact effective potentials and efficient, shared-exponent basis sets for the third-, fourth-, and fifth-row atoms, *Can. J. Chem.* **1992**, *70*, 612-630.
- [30] Krishnan, R.; Binkley, J.S.; Seeger, R.; Pople, J.A. Self-consistent molecular orbital methods. XX. A basis set for correlated wave functions, *J. Chem. Phys.* **1980**, *72*:650-654.

Sample Availability: Samples of the compounds are available from the authors.



© 2016 by the authors; licensee *Preprints*, Basel, Switzerland. This article is an open access article distributed under the terms and conditions of the Creative Commons by Attribution (CC-BY) license (<http://creativecommons.org/licenses/by/4.0/>).